Electronic Supplementary Material (ESI) for Inorganic Chemistry Frontiers.
This journal is © the Partner Organisations 2018

Supporting Information

Tailoring Yolk-Shell FeP@Carbon Nanoboxes with Engineered Void Space for Pseudocapacitance-Boosted Lithium Storage

Qiong Wang,[a] Boya Wang,[b] Zhi Zhang,[c] Yin Zhang,[a] Peng Jing,[a] Yun Zhang[b] and Hao Wu,[a]*

[a] College of Materials Science and Engineering, Sichuan University, Chengdu, P. R. China

[b] Department of Advanced Energy Materials, Sichuan University, Chengdu, P. R. China

[c]Center for Nanoscale Characterization and Devices, Wuhan National Laboratory for Optoelectronics, School of Physics, Huazhong University of Science and Technology, Wuhan, P. R. China

* **Corresponding authors**. E-mail: hao.wu@scu.edu.cn

Supporting Figures and Tables

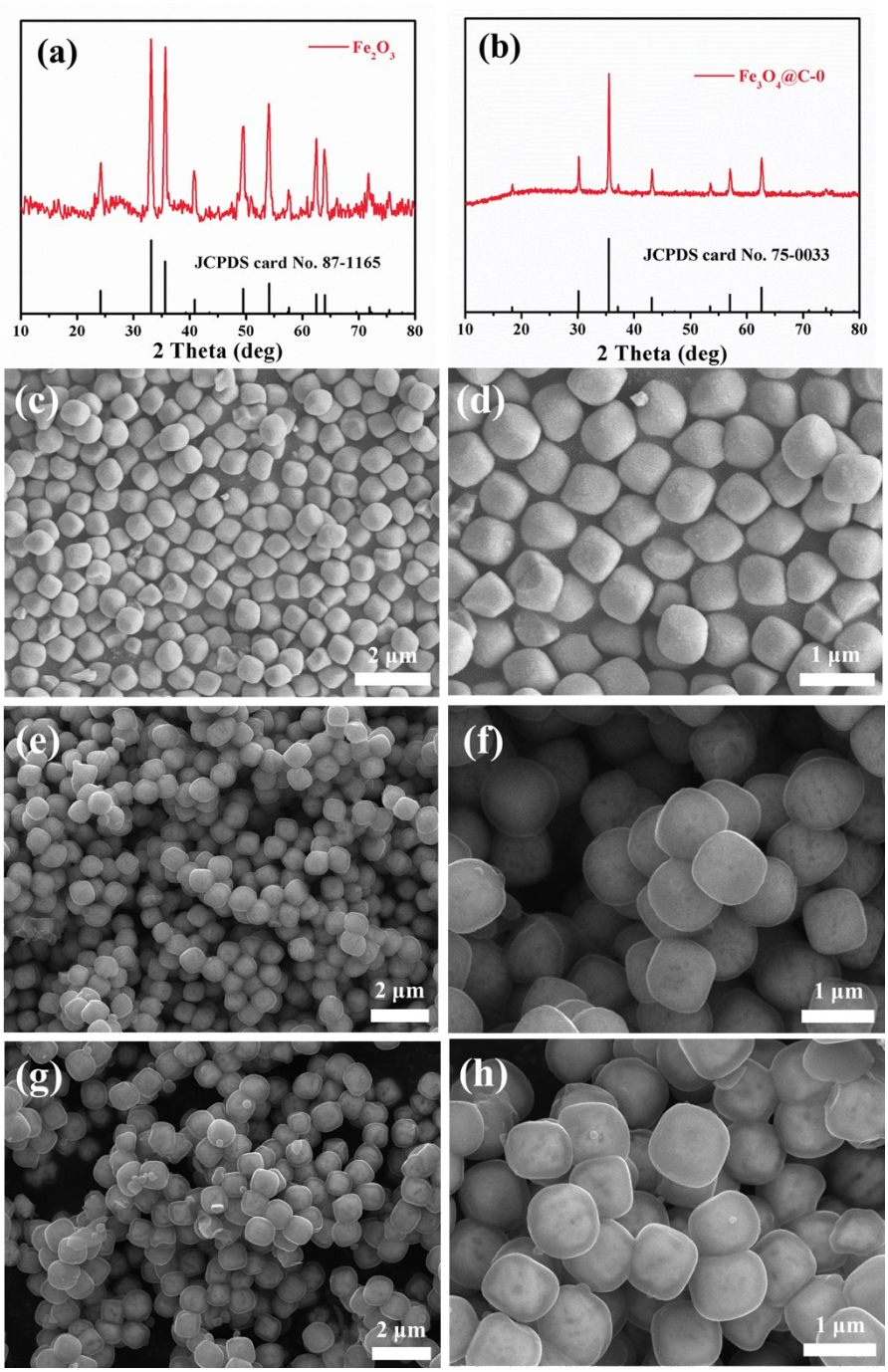

Figure S1 XRD patterns of a) Fe_2O_3 nanocubes and b) Fe_3O_4@C nanocubes; SEM images of c, d) Fe_2O_3 nanocubes, e, f) core-shell Fe_3O_4@C nanocubes, and g, h) yolk-shell Fe_3O_4@C nanoboxes.

The detailed counting process of carbon content:

Based on the TGA results, the weight content of carbon in samples were estimated as follows:

$$FeP \rightarrow 1/2\ Fe_2O_3 + 1/2\ P_2O_5$$

$$(1\text{-}x)\quad 0.92\ (1\text{-}x)\quad 0.82\ (1\text{-}x)$$

According to the previous reports, the FeP was finally oxidized to form Fe_2O_3 and P_2O_5 after TGA test under air atmosphere. Assuming the carbon content is x and the total mass is 1, thus the weight fractions for carbon can be calculated using the following formula:

$$\text{YS-FeP@C: } 0.92\ (1 - x) + 0.82\ (1 - x) – x = 118\ \%$$

$$\text{CS-FeP@C: } 0.92\ (1 - x) + 0.82\ (1 - x) – x = 126\ \%$$

Therefore, the carbon content in the YS-FeP@C and CS-FeP@C is estimated to be 20.2 % and 17.4 %, respectively.

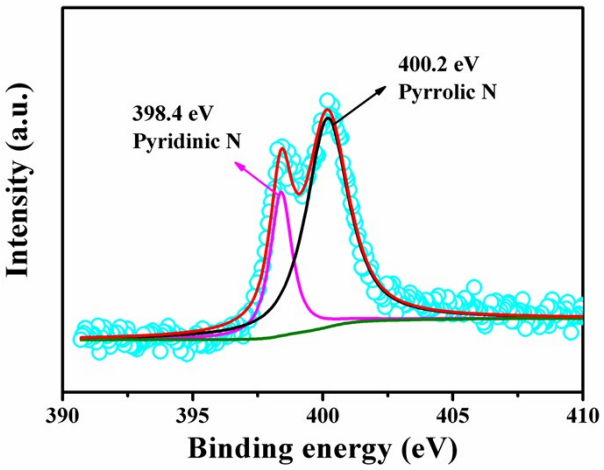

Figure S2 The high-resolution N 1s XPS spectra of YS-FeP@C.

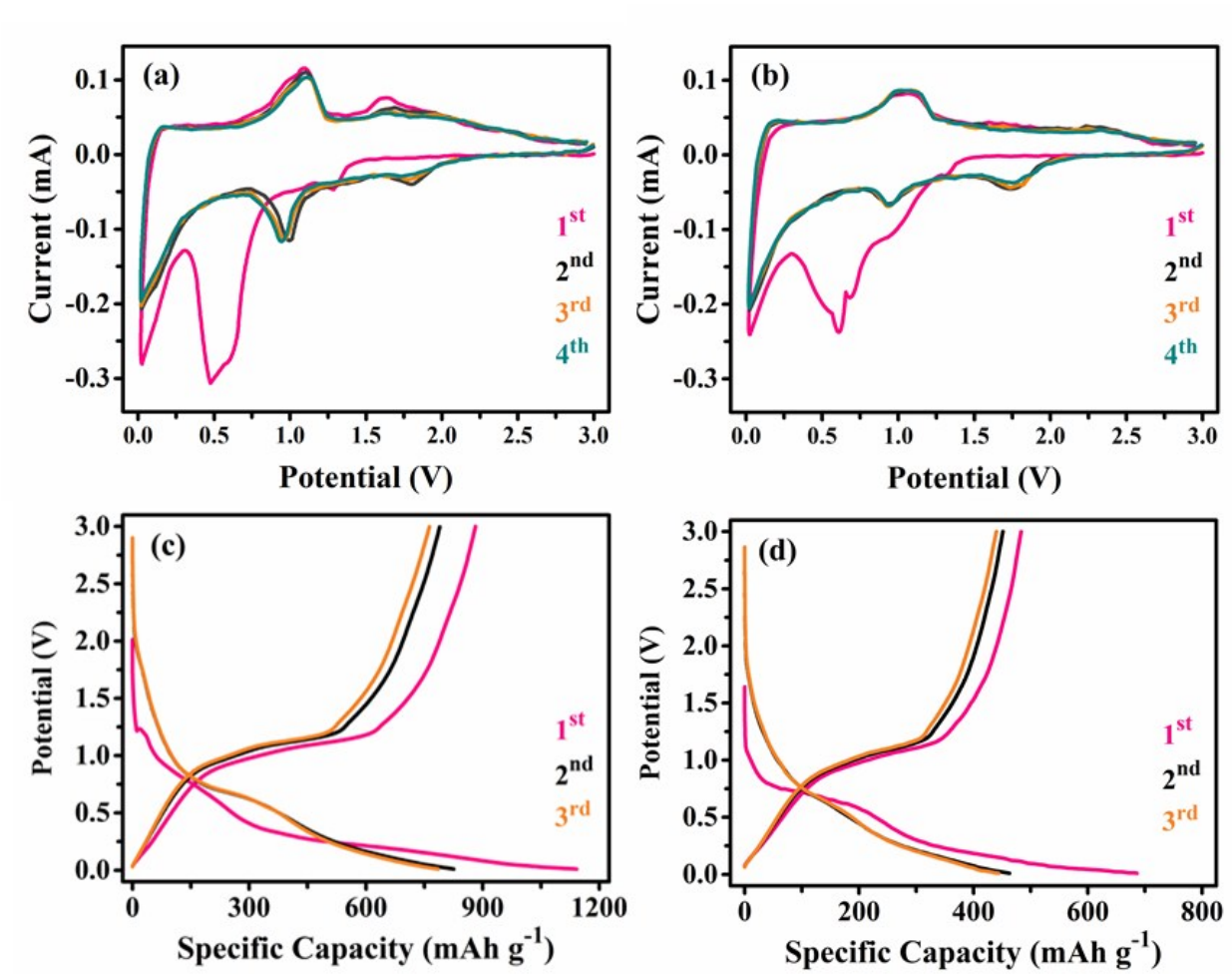

Figure S3 CV curves of a) YS-FeP@C and b) CS-FeP@C; Selected charge-discharge curves for the initial three cycles of c) YS-FeP@C and d) CS-FeP@C at a current density of 0.1 A g^{-1}.

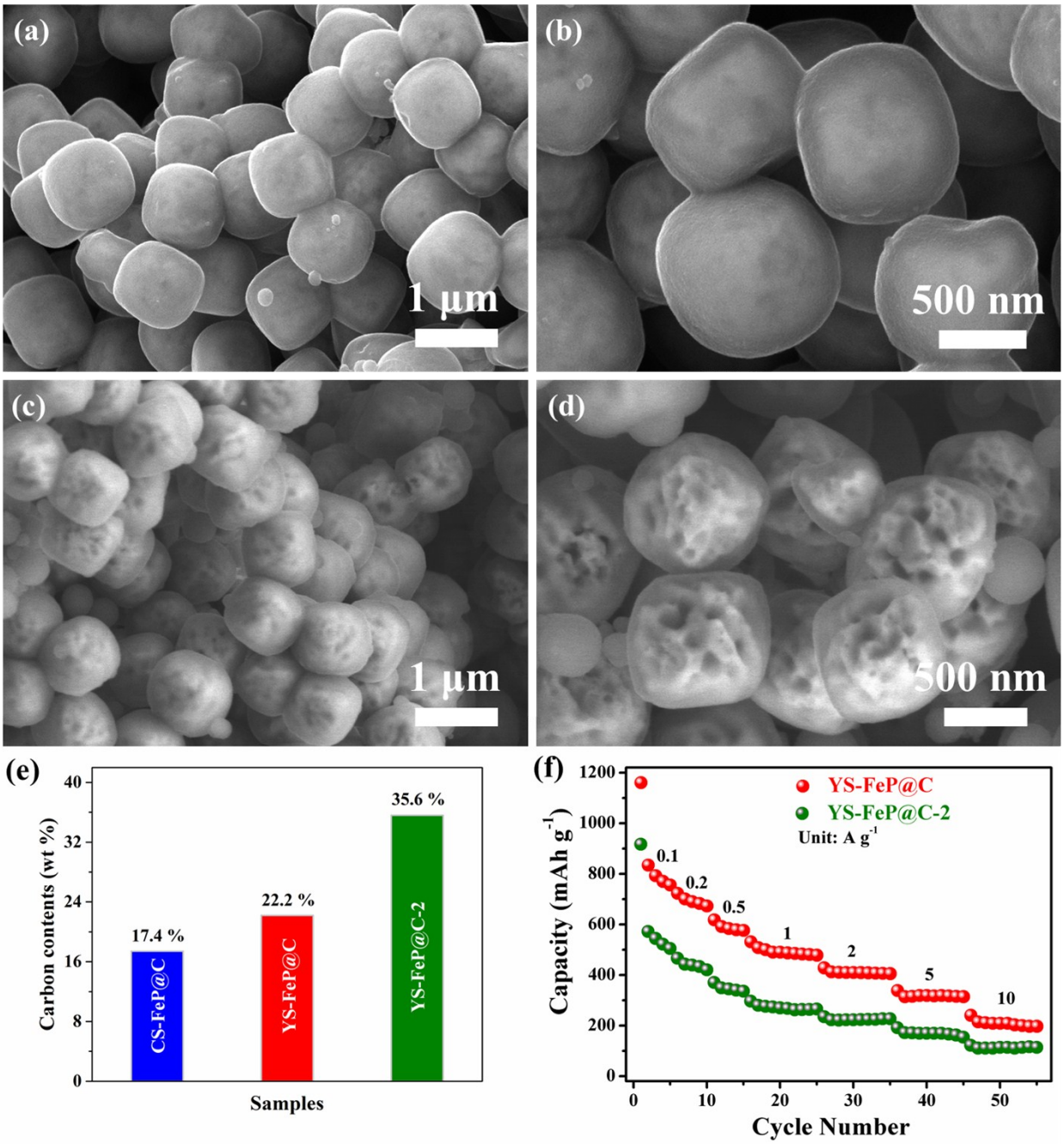

Figure S4 SEM images of a, b) YS-FeP@C and c, d) YS-FeP@C-2; e) The result of carbon content for all three samples; f) Rate performance comparison between YS-FeP@C and YS-FeP@C-2 electrodes from 0.1 to 10.0 A g^{-1}.

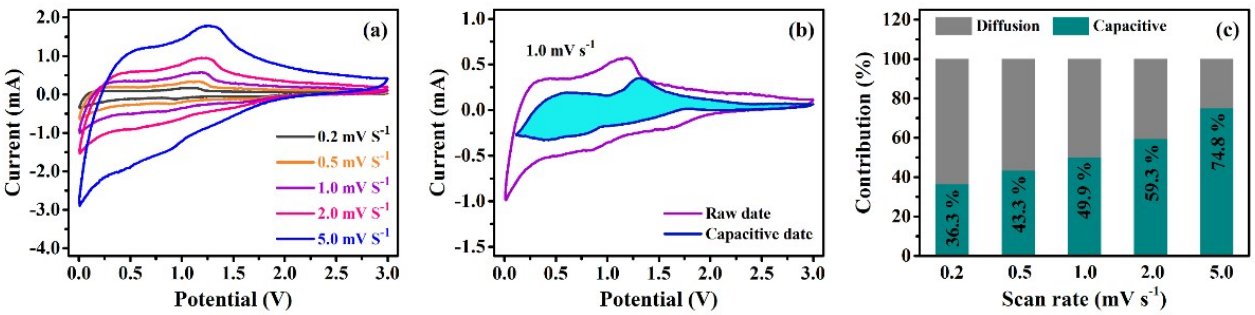

Figure S5 a) CV curves of CS-FeP@C electrode at various scan rates from 0.2 to 5.0 mV s^{-1}; b) Capacitive contribution of CS-FeP@C electrode at a scan rate of 1.0 mV s^{-1}; c) Contribution ratio of the capacitive and diffusion-controlled capacity versus scan rate of CS-FeP@C electrode.

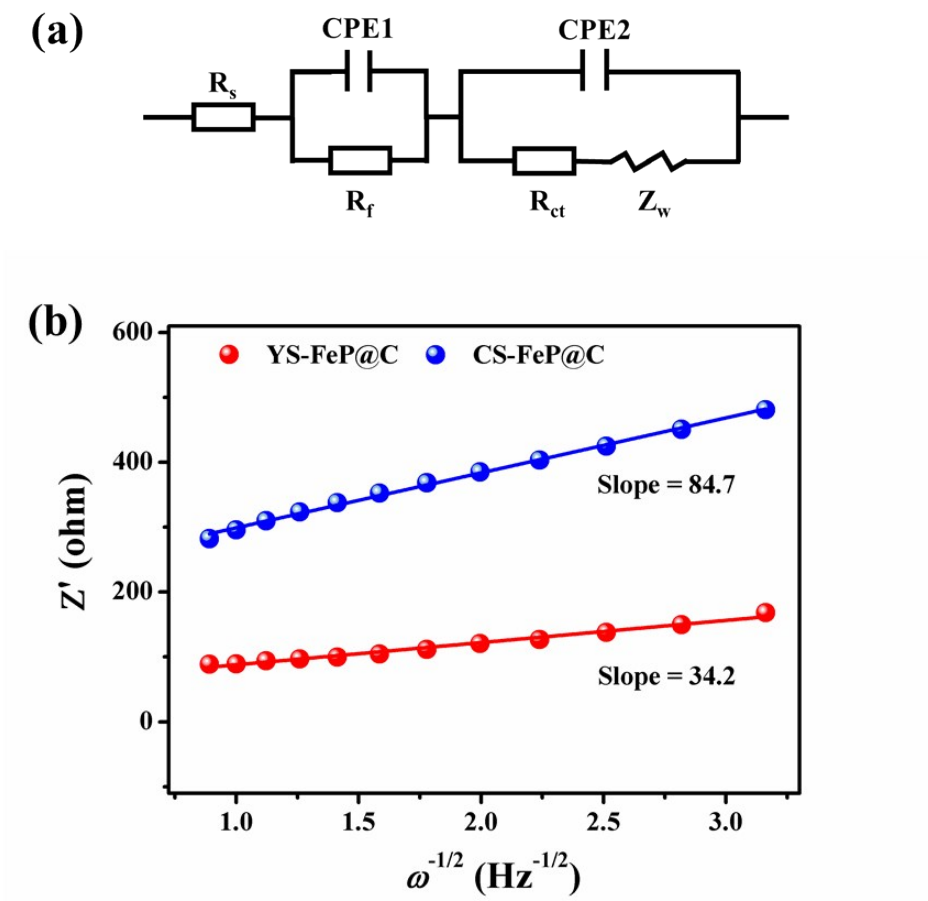

Figure S6 a) Equivalent circuit model for FeP@C composites; b) the Z'-$\omega^{-1/2}$ curves of YS-FeP@C and CS-FeP@C electrodes in the low-frequency region.

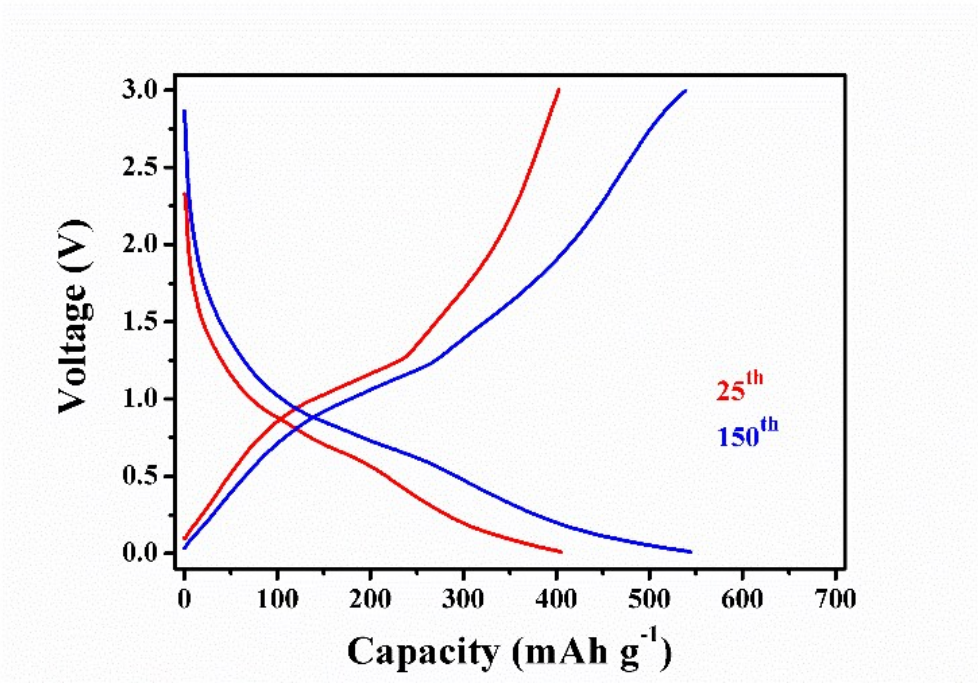

Figure S7 The charge-discharge curves for 25th and 150th cycles of YS-FeP@C at a current density of 1.0 A g^{-1}.